Development 138, 1161-1172 (2011) doi:10.1242/dev.057620

Genetic mosaic analysis reveals a major role for frizzled 4 and frizzled 8 in controlling ureteric growth in the developing kidney

Xin Ye[1,*], Yanshu Wang[1,2], Amir Rattner[1] and Jeremy Nathans[1,2,3,4,†]

SUMMARY

The developing mammalian kidney is an attractive system in which to study the control of organ growth. Targeted mutations in the Wnt receptors frizzled (Fz) 4 and Fz8 lead to reduced ureteric bud growth and a reduction in kidney size, a phenotype previously reported for loss of Wnt11. In cell culture, Fz4 and Fz8 can mediate noncanonical signaling stimulated by Wnt11, but only Fz4 mediates Wnt11-stimulated canonical signaling. In genetically mosaic mouse ureteric buds, competition between phenotypically mutant *Fz4*$^{-/-}$ or *Fz4*$^{-/-}$;*Fz8*$^{-/-}$ cells and adjacent phenotypically wild-type *Fz4*$^{+/-}$ or *Fz4*$^{+/-}$;*Fz8*$^{-/-}$ cells results in under-representation of the mutant cells to an extent far greater than would be predicted from the size reduction of homogeneously mutant kidneys. This discrepancy presumably reflects the compensatory action of a network of growth regulatory systems that minimize developmental perturbations. The present work represents the first description of a kidney phenotype referable to one or more Wnt receptors and demonstrates a general strategy for revealing the contribution of an individual growth regulatory pathway when it is part of a larger homeostatic network.

KEY WORDS: Fz4, Fz8, Kidney development, Wnt11, Wnt signaling, Organ size control, Mouse

INTRODUCTION

Multicellular organisms are characterized not only by the appropriate specification and spatial arrangement of diverse cell types but also by precise control of their relative abundances. At a macroscopic level, the latter feature is reflected in a match between overall body growth and the growth of individual organs and the substructures within those organs. Derangements in the control of cell proliferation that manifest as cancer generally require a large number of genetic alterations, providing evidence for a complex web of redundant and cross-regulating control systems (Weinberg, 2006). In the context of normal development, genetic perturbations that alter the rates of cell proliferation or death have been most sensitively revealed by situations in which the normal and modified cells compete for the same niche. Examples include competition between wild-type (WT) and *minute* cells in *Drosophila* imaginal discs (Martín and Morata, 2006; Neto-Silva et al., 2009), between cells with different active X-chromosomes in females heterozygous for X-linked dyskeratosis congenita (Vulliamy et al., 1997; Migeon, 1998), and between WT and severe combined immunodeficiency (SCID) cells in a bone marrow transplantation model (Otsu et al., 2000). Although the major regulators of cell proliferation, including the FGF, EGF, Hedgehog, TGFβ, Wnt and Hippo pathways, are now relatively well defined, the mechanisms by which these pathways interact to precisely regulate organ size are still largely unexplored.

[1]Department of Molecular Biology and Genetics, Johns Hopkins University School of Medicine, Baltimore, MD 21205, USA. [2]The Howard Hughes Medical Institute, Johns Hopkins University School of Medicine, Baltimore, MD 21205, USA. [3]Department of Neuroscience, Johns Hopkins University School of Medicine, Baltimore, MD 21205, USA. [4]Department of Ophthalmology, Johns Hopkins University School of Medicine, Baltimore, MD 21205, USA.

*Present address: Whitehead Institute for Biomedical Research, Cambridge, MA 02142, USA
[†]Author for correspondence (jnathans@jhmi.edu)

Accepted 29 December 2010

The developing mammalian kidney is an attractive system in which to study epithelial-mesenchymal interactions, the local determination of cell fates and the control of cell proliferation (Dressler, 2009). The ratio of kidney size to body size critically affects renal function and homeostasis, as clinical studies indicate that even a small reduction in nephron number significantly increases the risks for renal failure and hypertension (Brenner et al., 1997; Giral et al., 2010). The earliest events in kidney development are the invasion of the metanephric mesenchyme by the ureteric bud and the subsequent growth and branching of the bud epithelium. Gdnf, a major regulator of bud growth, is produced by the mesenchyme and acts on the bud epithelium via the Ret tyrosine kinase receptor and Gfra1 co-receptor (Hellmich, 1996; Costantini and Shakya, 2006). Gdnf signaling is regulated at multiple levels. Sprouty 1 (Spry1), an intracellular kinase antagonist, inhibits Ret signaling in the bud epithelium (Chi et al., 2004; Basson et al., 2006). Wnt11, produced by the bud, increases *Gdnf* transcription, which, in turn, activates *Wnt11* transcription (Majumdar et al., 2003). Two other Wnts, Wnt4 and Wnt9b, play major roles in the mesenchymal-to-epithelial transition that is required for the formation of renal vesicles (Stark et al., 1994; Carroll et al., 2005). Angiotensin 2, BMP, FGF, retinoic acid (RA) and TGFβ signaling pathways also regulate branching morphogenesis and growth by the ureteric bud (Godin et al., 1999; Oxburgh et al., 2004; Grieshammer et al., 2005; Bates, 2007; Dressler, 2009; Rosselot et al., 2010; Song et al., 2010).

Wnt ligands act through multiple families of receptors and co-receptors to induce changes in gene transcription (canonical Wnt signaling) or in the cytoskeleton (noncanonical Wnt signaling) (van Amerongen and Nusse, 2009). The canonical Wnt signal funnels through β-catenin, but noncanonical Wnt signaling involves pathways that are still poorly understood. In mammals there are ten seven-pass Frizzled receptors and two single-pass Lrp co-receptors. Frizzled proteins can mediate both canonical signaling in collaboration with Lrp co-receptors and noncanonical signaling,

although it appears likely that some Frizzleds mediate only one or the other type of signaling. Wnts can also signal through the Ryk and ROR transmembrane tyrosine kinase receptors. At present, the receptors that mediate Wnt signaling in kidney development are unknown, and the signaling pathways that they activate are poorly defined.

In the present work, we describe a phenotype of reduced ureteric bud growth and a reduction in kidney size in the absence of Frizzled (Fz; or Fzd) 4 and Fz8. This phenotype, together with cell culture analyses of Wnt11 signaling via Fz4 and Fz8, suggests that these two receptors might mediate some or all of the actions of Wnt11 in the mouse kidney. Using genetically mosaic buds, we further show that when phenotypically mutant *Fz4*$^{-/-}$ or *Fz4*$^{-/-}$;*Fz8*$^{-/-}$ cells compete with adjacent phenotypically WT *Fz4*$^{+/-}$ or *Fz4*$^{+/-}$;*Fz8*$^{-/-}$ cells, respectively, the mutant cells become under-represented to a far greater extent than would be predicted from the more modest growth retardation of non-mosaic kidneys. This work represents the first description of a kidney phenotype that is referable to the genetic ablation of one or more Wnt receptors, and it indicates that Frizzled signaling is a major regulator of kidney size during development. The genetic mosaic experiment also demonstrates a general strategy for revealing the contribution of individual growth regulatory pathways when they are part of a larger homeostatic network.

MATERIALS AND METHODS

Production of *Fz8* knockout mice

The *Fz8* knockout (KO) allele was created by standard gene-targeting methods (see Fig. S1 in the supplementary material). The targeting vector was introduced by electroporation into R1 embryonic stem (ES) cells and plated in medium containing G418 and ganciclovir. ES colonies were screened for the correct targeting event by Southern blot hybridization with flanking probes, and targeted cells were injected into C57BL/6 blastocysts. Germline transmission was confirmed by Southern blot hybridization. Mice were housed and handled in accordance with protocols approved by the Johns Hopkins University Animal Care and Use Committee and the IACUC guidelines.

Genotyping

PCR primers (5′ to 3′) for *Fz8* genotyping were *Fz8* KO (sense strand, CTCCCTTTTCTCAGATTCCTCACTGCAGAGCCCT; antisense strand, CATCAACATTAAATGTGAGCGAGTAACAACCCG; product size, ~500 bp) and *Fz8* WT (sense strand, as *Fz8* KO; antisense strand, GCACTGTATCTCCACCAGCGGCCAA; product size, 320 bp). DNA was extracted using the REDExtract-N-Amp Tissue PCR Kit (Sigma). PCR was performed with 35 cycles of denaturation at 94°C for 30 seconds, annealing at 60°C for 30 seconds, and elongation at 72°C for 30 seconds. PCR genotyping of the *Tie2Cre*, *R26CreER* and the various *Fz4* alleles was as described (Wang et al., 2001; Badea et al., 2003; Ye et al., 2009).

Histochemistry and immunostaining

For alkaline phosphatase (AP) histochemistry, whole-mount kidneys and brain sections were processed and stained with nitroblue tetrazolium/5-bromo-4-chloro-indolyl phosphate (NBT/BCIP) as described (Badea et al., 2003). Endogenous AP activity was eliminated by heating the tissue to 68°C for 90 minutes. Immunostaining was performed following AP histochemistry when needed. For X-gal staining, E11.5 kidneys were dissected and fixed for 10 minutes at room temperature in 2.5% paraformaldehyde, 0.2% glutaraldehyde in PBS with 2 mM $MgCl_2$, and incubated in X-gal staining solution overnight at 37°C. For Hematoxylin and Eosin staining, kidneys from E18.5 embryos were fixed in Carnoy's solution overnight and then dehydrated through a graded alcohol series before embedding in paraffin. Sections were cut at 8 μm. For whole-mount immunostaining, kidneys were fixed in 4% paraformaldehyde for 1 hour at room temperature, rinsed with PBS, and incubated with the primary antibodies rat anti-E-cadherin (1:400; Abcam) and rabbit anti-Pax2 (1:200; Abcam) at 4°C overnight. After 5 washes with PBST (0.3% Triton X-100 in PBS), the tissue was incubated with secondary antibodies at 4°C overnight, washed three times with PBST, and mounted in Fluoromount G (Southern Biotech).

To detect cell proliferation, 60 μg/g body weight bromodeoxyuridine (BrdU) or 25 μg/g body weight 5-ethynyl-2′-deoxyuridine (EdU) was injected intraperitoneally into pregnant females at the indicated gestational ages. One hour after injection, embryos were harvested and the kidneys dissected and fixed in 4% paraformaldehyde for 2 hours at room temperature (BrdU; E15.5 kidneys) or in 2% paraformaldehyde for 1 hour at room temperature (EdU; E12.5 kidneys). For BrdU, fixed kidneys were equilibrated with 30% sucrose in PBS, and mutant and control kidneys from the same litter were embedded together in one block for preparation of frozen sections. Kidney sections were treated in 2M HCl for 20 minutes and subjected to double immunostaining with antibodies against calbindin [1:1000 rabbit anti-calbindin D-28K (Swant)] and BrdU [1:200 rat anti-BrdU (Abcam)]. For EdU, fixed kidneys were incubated overnight at 4°C in rabbit anti-calbindin antibody in PBS containing 10% normal goat serum and 0.5% Triton X-100, washed in PBS containing 0.5% Triton X-100 for 8 hours with hourly changes of solution, and then incubated overnight at 4°C in Alexa Fluor 488 goat anti-rabbit antibody (1:400 in PBS containing 10% normal goat serum and 0.5% Triton X-100). The kidneys were extensively washed again before in situ EdU detection using the azide alkyne Huisgen cycloaddition reaction (Salic and Mitchison, 2008) (Click-iT, Invitrogen). To detect cell death, kidney sections were double stained with antibodies against cleaved caspase 3 [1:300 rabbit anti-cleaved caspase 3 (Cell Signaling)] and E-cadherin. Secondary antibodies were purchased from Invitrogen.

4-hydroxytamoxifen treatment

To obtain ~50% recombination, 200 μg 4-hydroxytamoxifen (4HT; H6278, Sigma) was injected into the neck fat pad of pregnant females at E8.5. To achieve ~90% recombination, pregnant females were orally gavaged with ~1 mg 4HT (H7904, Sigma) at E8.5.

In situ hybridization

In situ probe templates for riboprobe synthesis were obtained from the following sources: *Ret* was a gift from Drs Wenqin Luo and David Ginty (John Hopkins Medical School, MD, USA); *Six2* was a gift from Dr Aurora Esquela (Eastern Virginia Medical School, VA, USA); *Gdnf*, *Slc12a3* and *Slc34a1* cDNA clones (Open Biosystems) were used without modification; *Wnt4* and *Wnt11* coding regions were PCR amplified from cDNA clones (Open Biosystems) and subcloned into pBS; and uromodulin (*Umod*) exon 3 was PCR amplified from genomic DNA and subcloned into pBS.

Whole-mount (Grieshammer et al., 2005) and tissue (Schaeren-Wiemers and Gerfin-Moser, 1993) in situ hybridization were performed as described. For *Gdnf* whole-mount in situ hybridization experiments, mutant and control kidneys were processed together during the entire protocol to ensure that they were exposed to identical experimental conditions. Mutant and control kidneys were distinguished based on attachment to half a gonad (mutant kidneys) or the entire gonad (control kidneys). After color development, kidneys were dissected away from the gonad, rinsed in PBST, post-fixed in 4% paraformaldehyde and cleared in 75% glycerol.

Canonical and noncanonical Wnt signaling assays

Luciferase reporter-based canonical Wnt signaling assays were performed as previously described using the Super Top Flash cell line (Xu et al., 2004). Rho activation was assayed with the Rho Activation Kit from Roche (#17-294) following the manufacturer's instructions. The two Rho kinase inhibitors Y-27632 and H-1152P were purchased from Calbiochem (#688001 and #555552).

Microarray hybridization and data analysis

RNA was isolated using Trizol (Invitrogen) and the RNeasy Kit (Qiagen). For microarray hybridization, RNA samples were labeled with the Ovation RNA Amplification System V2 (#3100; for ~0.2-1 μg RNA samples) and FL-Ovation cDNA Biotin Module V2 (#4200) Kits (Nugen). The labeled probes were hybridized to Affymetrix MOE 430 2.0 chips, which have more than 45,000 probe sets representing ~34,000 genes, providing essentially

complete coverage of known and predicted mouse protein-coding genes. Microarray data were analyzed with Spotfire software. Microarray data are deposited at Gene Expression Omnibus under accession numbers GSE23781 and GSE26668.

Statistics

P-values were calculated with Student's *t*-test (Microsoft Excel) or with Spotfire software for microarray data.

RESULTS

Renal hypoplasia in *Fz4*$^{-/-}$ and *Fz4*$^{-/-}$;*Fz8*$^{-/-}$ mice

As part of a systematic analysis of Frizzled function in vivo, we generated a targeted mutation in the mouse *Fz8* gene by replacing its open reading frame with an *E. coli* β-galactosidase (*lacZ*) open reading frame and *PGK-neo* selection cassette (see Fig. S1 in the supplementary material). Since *Fz8*$^{-/-}$ mice show no defects in viability, size or fertility, we explored the possibility that *Fz8* might function redundantly with one or more of the nine other Frizzled genes. In keeping with this idea, we observed that *Fz4*$^{-/-}$;*Fz8*$^{-/-}$ mice exhibit postnatal lethality with 100% penetrance, with no *Fz4*$^{-/-}$;*Fz8*$^{-/-}$ weanlings among 141 postnatal day (P) 14 animals, in which this genotype should have constituted 25% of the mice. By contrast, when litters from the same crosses were harvested at E18.5, *Fz4*$^{-/-}$;*Fz8*$^{-/-}$ fetuses were found at the expected Mendelian frequency with no outward phenotypes.

Fz4 and *Fz8* showed nearly identical patterns of expression within the developing kidney as determined by expression of a *lacZ* reporter inserted at each locus (Fig. 1A-G). Both genes were expressed in the developing ureteric buds as early as E11.5, and expression was observed not only in the collecting system but also in the nephron epithelia until at least E15.5. After this time point, endogenous β-galactosidase enzyme activity within the kidney partially obscured the histochemical analysis of gene-targeted β-galactosidase activity. A second *Fz4* allele, in which the human placental alkaline phosphatase (AP) open reading frame replaces the *Fz4* open reading frame (Ye et al., 2009), revealed continuing expression of *Fz4* in the collecting system and nephron epithelia as late as E18.5 (Fig. 1H,I). These observations are consistent with whole-mount in situ hybridization analyses showing expression of *Fz4* and *Fz8* in the E15.5 kidney; *Fz2*, *Fz6*, *Fz7* and *Fz10* are also expressed at this time point (McMahon et al., 2008) (www.gudmap.org). The similar patterns of *Fz4* and *Fz8* expression described here suggested the possibility that these genes are functionally redundant during kidney development.

At E18.5, the only gross anatomic anomaly that distinguished *Fz4*$^{-/-}$;*Fz8*$^{-/-}$ fetuses from their control littermates was a linear reduction in kidney size of ~30% (equivalent to a ~65% reduction in volume; Fig. 1J-M,P). A ~20% linear reduction in kidney size was observed in *Fz4*$^{-/-}$;*Fz8*$^{+/-}$ fetuses, and a ~15% linear reduction was observed in *Fz4*$^{-/-}$ fetuses (Fig. 1P). Previously, we reported that *Fz4* is expressed in the vasculature throughout development and that vascular defects are observed in the retina, inner ear and cerebellum in *Fz4*$^{-/-}$ mice (Xu et al., 2004; Ye et al., 2009). However, the effect of *Fz4* deletion on kidney development appears to be independent of its function in the vasculature, as shown by the normal kidney size and postnatal survival of mice with selective deletion of the *Fz4* locus in the vasculature (*Fz4*$^{CKOAP/-}$;*Tie2Cre*; Fig. 1P). At present, we do not know whether renal insufficiency contributes to the postnatal lethality in *Fz4*$^{-/-}$;*Fz8*$^{-/-}$ mice or whether there are additional defects that play a more important role.

Strikingly, the internal architecture of the smaller *Fz4*$^{-/-}$;*Fz8*$^{-/-}$ kidneys at E18.5 appeared to be entirely normal at the light-microscope level, with morphologically normal glomeruli, proximal tubules, loops of Henle and collecting ducts, and no evidence of cysts (Fig. 1L-O). To assess nephron development in greater detail, E15.5 kidneys were analyzed by in situ hybridization for markers of nephron progenitors (*Six2*), pretubular aggregates (*Wnt4*), differentiated nephron structures including podocytes (i.e. glomeruli; *Podxl*), the thick ascending limb of the loop of Henle and early distal convoluted tubules (uromodulin), proximal convoluted tubules (*Slc34a1*) and distal convoluted tubules (*Slc12a3*). For each of these structures, the size, location and packing density appeared to be normal in the *Fz4*$^{-/-}$;*Fz8*$^{-/-}$ kidney (Fig. 2). Thus, the principal defect in the mutant kidney is a proportional reduction in organ size.

Decreased growth, branching and cell proliferation in *Fz4*$^{-/-}$;*Fz8*$^{-/-}$ ureteric buds

The ureteric bud serves as an important signaling center for differentiation of the nephrons, and the number of nephrons, as well as the ultimate size of the kidney, is determined by the growth of the ureteric bud (Dressler, 2009). The *Fz4*$^{-/-}$;*Fz8*$^{-/-}$ kidney phenotype described above suggests a deficiency in the proliferation and branching of the ureteric epithelium early in kidney development. To visualize the ureteric buds at the earliest stages in their branching, E-cadherin (a marker for ureteric epithelium) and Pax2 (a marker for metanephric mesenchyme), and *Ret* and *Wnt11* transcripts (markers for ureteric branch tips) were localized in whole-mount kidneys at E11.5. The E11.5 *Fz4*$^{-/-}$;*Fz8*$^{-/-}$ ureteric bud had invaded the metanephric mesenchyme, completed the first branching event and was only subtly smaller than the control *Fz4*$^{+/+}$;*Fz8*$^{-/-}$ bud (Fig. 3A-F). However, by E12.5, ureteric branching was clearly retarded in *Fz4*$^{-/-}$;*Fz8*$^{-/-}$ embryos (Fig. 3G-J).

Following the first branching event at E11.5, the ureteric epithelium proliferates extensively and undergoes many rounds of branching to form a complex ureteric tree. To determine whether the *Fz4*$^{-/-}$;*Fz8*$^{-/-}$ ureteric branching defect was accompanied by a decrease in cell proliferation and/or an increase in cell death, we examined E15.5 kidneys by BrdU pulse labeling and anti-cleaved caspase 3 immunostaining (Fig. 4A). These analyses showed a ~1.8-fold reduction in the density of BrdU-labeled cells in ureteric bud tips in *Fz4*$^{-/-}$;*Fz8*$^{-/-}$ compared with *Fz4*$^{+/+}$;*Fz8*$^{-/-}$ kidneys, a difference that was statistically highly significant (Fig. 4B). By contrast, there was no statistically significant difference in the number of BrdU-labeled cells in the renal pelvis, developing collecting ducts (defined as the medullary regions of the ureteric epithelium), or cortical mesenchyme at this stage (Fig. 4B), nor was there a statistically significant difference in the extremely low rate of cell death, as assessed either in ureteric bud tips or throughout the entire kidney (Fig. 4C). The overall cell density in the bud tips, as determined from the density of DAPI-stained nuclei, was similar between genotypes (Fig. 4C). A similar experiment performed at E12.5 using a 1-hour pulse of EdU showed an extremely high density of labeled nuclei in ureteric buds and mesenchyme in *Fz4*$^{+/+}$;*Fz8*$^{-/-}$, *Fz4*$^{+/-}$;*Fz8*$^{-/-}$ and *Fz4*$^{-/-}$;*Fz8*$^{-/-}$ kidneys (see Fig. S2 in the supplementary material). Although the high density of the labeled nuclei hindered precise quantification, by visual inspection the number of EdU-labeled nuclei within the ureteric buds was not dramatically different across the genotypes at this stage.

Genetic mosaic analysis reveals that Fz4 signaling is a major regulator of kidney size

The retarded development of *Fz4*$^{-/-}$ and *Fz4*$^{-/-}$;*Fz8*$^{-/-}$ kidneys described above occurs in the context of a complex network of growth regulatory signals that include Wnt, Gdnf/Ret/Gfra1,

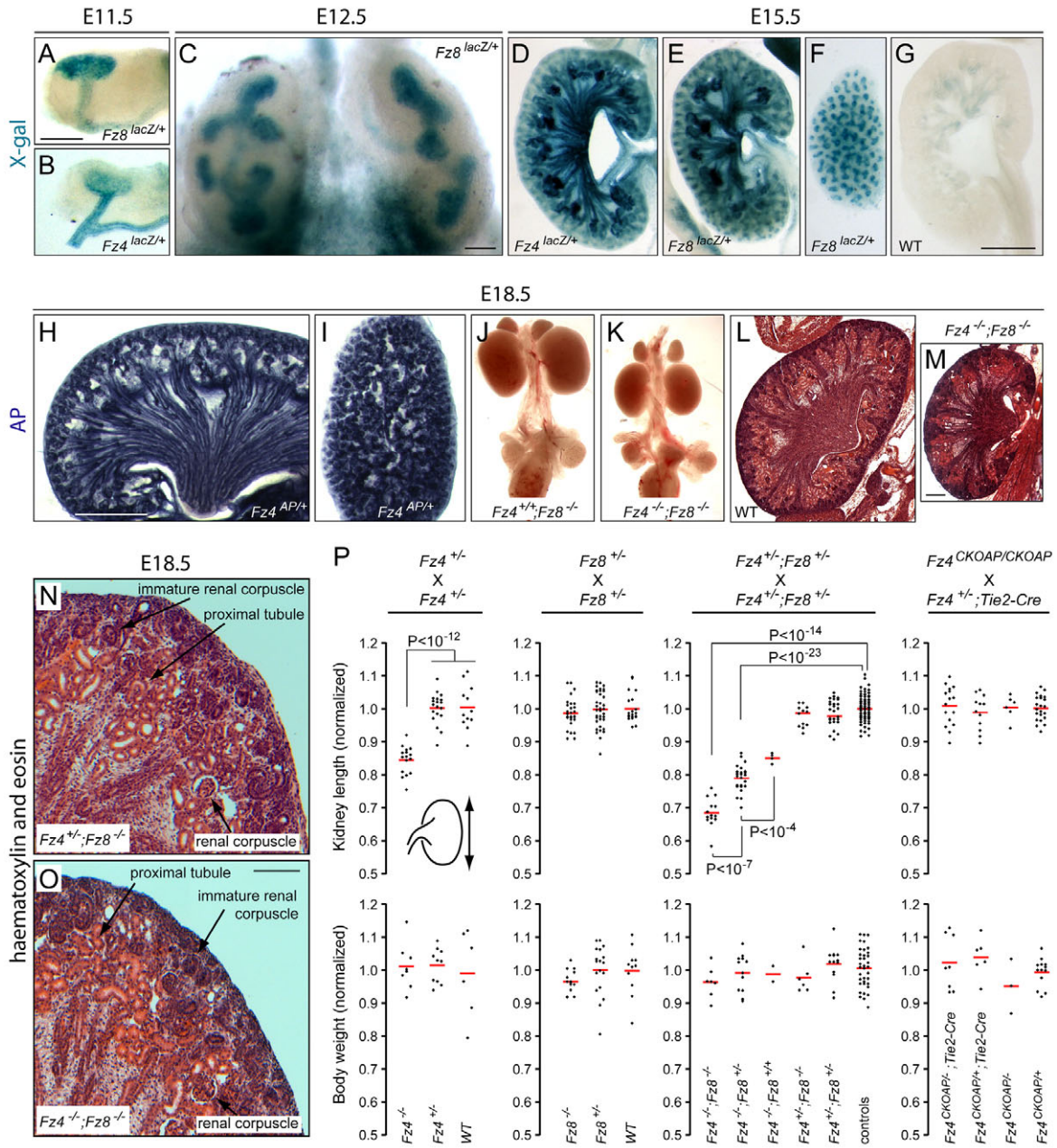

Fig. 1. Renal growth defects in *Fz4*$^{-/-}$ and *Fz4*$^{-/-}$;*Fz8*$^{-/-}$ mouse embryos. (**A-G**) X-gal staining (blue) shows expression of *Fz4*^{lacZ} and *Fz8*^{lacZ} in the ureteric buds at E11.5 and E12.5 (A-C), and in developing nephron epithelia and the collecting system at E15.5 (D-G). A-C show intact kidneys; D-G show 100 μm vibratome sections, with F showing a section at the cortical surface. (**H**,**I**) Alkaline phosphatase (AP) histochemistry of 100 μm vibratome sections from an E18.5 *Fz4*$^{AP/+}$ kidney shows expression throughout the nephron epithelia and collecting system. Wild-type (WT) kidney sections processed in parallel show no staining. (**J**,**K**) Dissected urogenital tracts at E18 show that loss of *Fz4* leads to a selective reduction in kidney size. The size of the *Fz4*$^{+/+}$;*Fz8*$^{-/-}$ control kidney is indistinguishable from that of the WT (as quantified in P). (**L-O**) The internal structure and organization of E18.5 *Fz4*$^{-/-}$;*Fz8*$^{-/-}$ kidneys (M,O) closely resemble those of the WT (L) and phenotypically WT *Fz4*$^{+/-}$;*Fz8*$^{-/-}$ (N) kidney at both a gross level (L,M; images are at the same magnification) and at the level of cellular organization (N,O). (**P**) Quantification of E18 kidney lengths (upper panels) and body weights (lower panels) for crosses that generated various combinations of *Fz4* and/or *Fz8* null alleles. See inset diagram defines kidney length. Length and weight values are normalized to those of WT and heterozygous littermates, or, for the crosses between *Fz4*$^{+/-}$;*Fz8*$^{+/-}$ parents (third column), to a control group consisting of all *Fz4*$^{+/+}$ littermates regardless of *Fz8* genotype as well as *Fz4*$^{+/-}$;*Fz8*$^{+/+}$ littermates. Red horizontal bars show the mean. Scale bars: 200 μm for A,B,L,M; 100 μm for C,N,O; 500 μm for D-I.

FGF, RA and BMP pathways. If negative-feedback mechanisms exist between pathways then one might expect that the phenotypic consequences of a defect in one growth-promoting pathway could be partially masked by the compensatory activation of other pathways. To reveal the intrinsic strength of the Fz4 and Fz8 signaling pathway, we designed a tissue mosaic experiment to quantify the relative efficiencies with which genetically marked *Fz4*$^{-/-}$;*Fz8*$^{-/-}$ versus *Fz4*$^{+/-}$;*Fz8*$^{-/-}$ or *Fz4*$^{-/-}$ versus *Fz4*$^{+/-}$ epithelial cells populate the same developing ureteric buds.

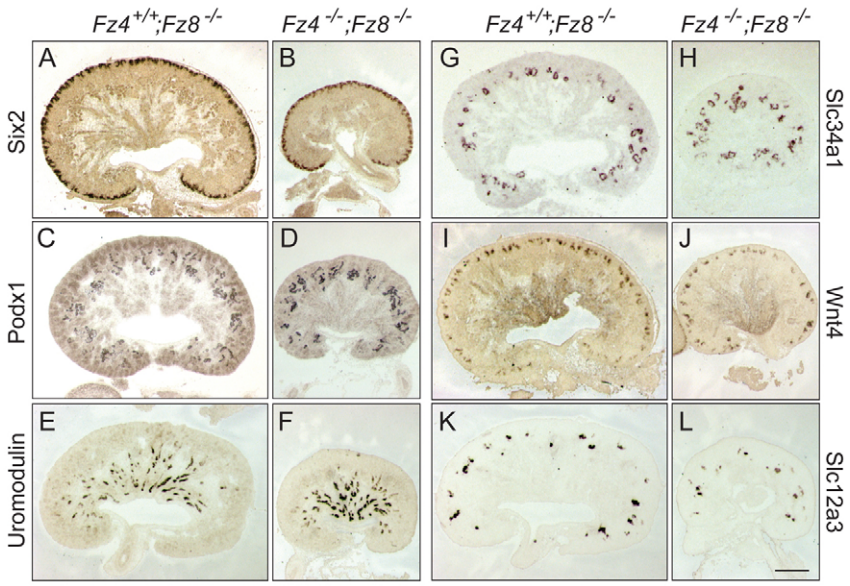

Fig. 2. Normal differentiation of E15 *Fz4*$^{-/-}$;*Fz8*$^{-/-}$ kidneys as determined with molecular markers. (**A-L**) In situ hybridization for the indicated transcripts shows a normal density and arrangement of nephron progenitors (*Six2*), podocytes (i.e. glomeruli; *Podx1*), the thick ascending limb of the loop of Henle and early distal convoluted tubules (uromodulin), proximal convoluted tubules (*Slc34a1*), pretubular aggregates (*Wnt4*) and distal convoluted tubules (*Slc12a3*) in *Fz4*$^{-/-}$;*Fz8*$^{-/-}$ versus *Fz4*$^{+/+}$;*Fz8*$^{-/-}$ mouse kidneys at E15. Scale bar: 400 μm.

In this experiment, Cre-mediated recombination converts a conditional *Fz4* allele with a downstream but unexpressed AP reporter coding region (*Fz4*^{CKOAP}) into a null allele that lacks Fz4 coding and 3′ UTR sequences and expresses the AP reporter under the control of the *Fz4* promoter (*Fz4*^{AP}) (Ye et al., 2009) (see Fig. S3 in the supplementary material). When the *Fz4*^{CKOAP} allele is paired with a WT *Fz4* allele (*Fz4*$^{CKOAP/+}$) or a conventional *Fz4* null allele (*Fz4*$^{CKOAP/-}$), Cre-mediated recombination generates AP-expressing cells that are either phenotypically WT (*Fz4*$^{AP/+}$) or mutant (*Fz4*$^{AP/-}$), respectively. To create a fine-grained mosaic of mutant and WT cells, 4-hydroxytamoxifen (4HT) was administered at E8.5 to activate Cre-mediated recombination via a ubiquitously expressed *CreER* at the *ROSA26* locus (*R26CreER*). We note that the crosses used in this experiment – *Fz4*$^{CKOAP/CKOAP}$ × *Fz4*$^{+/-}$;*R26CreER/R26CreER* and *Fz4*$^{CKOAP/CKOAP}$;*Fz8*$^{-/-}$ × *Fz4*$^{+/-}$;*Fz8*$^{-/-}$;*R26CreER/R26CreER* – generate, on average, a 1:1 ratio of experimental and control embryos within the same litter.

At E12.5, kidneys were histochemically stained for AP, the ureteric epithelium was visualized by immunostaining for calbindin, and the distal branches with and without AP^{+} cells were counted (Fig. 5). As seen in Fig. 5A, cells that lack *Fz4* expression were dramatically under-represented in the ureteric epithelium as judged by quantifying the number of terminal branches populated by AP^{+} cells. This difference, which is of high statistical significance, was seen in both *Fz8*$^{+/+}$ and *Fz8*$^{-/-}$ backgrounds. At the dose of 4HT used here (200 μg), the control kidneys showed that *Fz4*$^{AP/+}$ cells account for ~50% of the ureteric epithelial cells and populate over 80% of the distal branches. The failure of *Fz4*$^{AP/-}$ and *Fz4*$^{AP/-}$;*Fz8*$^{-/-}$ cells to populate the mosaic ureteric epithelium indicates that Fz4/Fz8 signaling is a major regulator of ureteric epithelial growth. Similar experiments in which more than 10 litters were examined following 4HT delivery at E13.5 resulted in variably smaller kidneys at E18.5, indicating an ongoing requirement for *Fz4* and *Fz8* function during later kidney development (data not shown).

An important assumption in the genetic mosaic experiment is that experimental and control embryos are exposed to equal levels of 4HT and undergo equal frequencies of Cre-mediated recombination. As 4HT was delivered subcutaneously in the cervical fat pad of the mother, we would expect that transport of 4HT via the maternal circulatory system would result in equal exposure among the embryos within each litter. In several experiments, we directly examined Cre-mediated recombination in extra-renal tissues by AP histochemical staining, and, as shown in Fig. 5B and Fig. S4 in the supplementary material, similar levels of Cre-mediated recombination were found in experimental

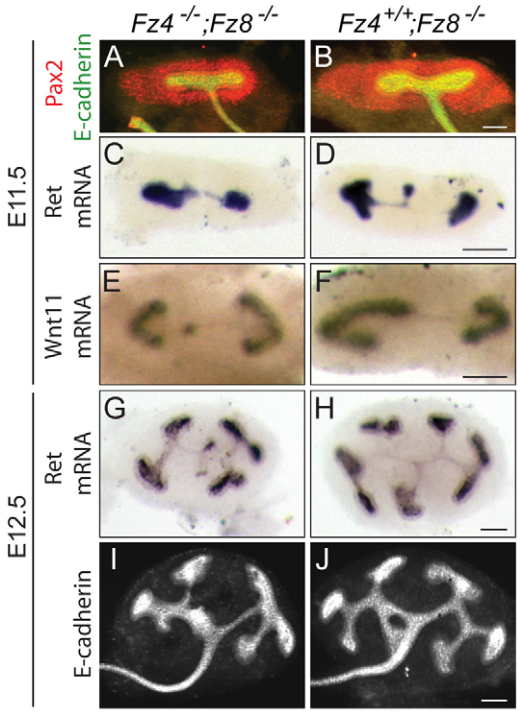

Fig. 3. Retarded growth and branching of ureteric buds in *Fz4*$^{-/-}$;*Fz8*$^{-/-}$ mouse kidneys. (**A-F**) At E11.5, immunolocalization of Pax2 and E-cadherin (A,B) and in situ localization of *Ret* and *Wnt11* transcripts (C-F) reveal retarded growth of ureteric buds in the *Fz4*$^{-/-}$;*Fz8*$^{-/-}$ kidney. (**G-J**) At E12.5, there is impoverished branching of ureteric buds in the *Fz4*$^{-/-}$;*Fz8*$^{-/-}$ kidney. *Fz4*$^{-/-}$;*Fz8*$^{-/-}$ and *Fz4*$^{+/+}$;*Fz8*$^{-/-}$ littermate samples were processed in parallel. Scale bars: 100 μm.

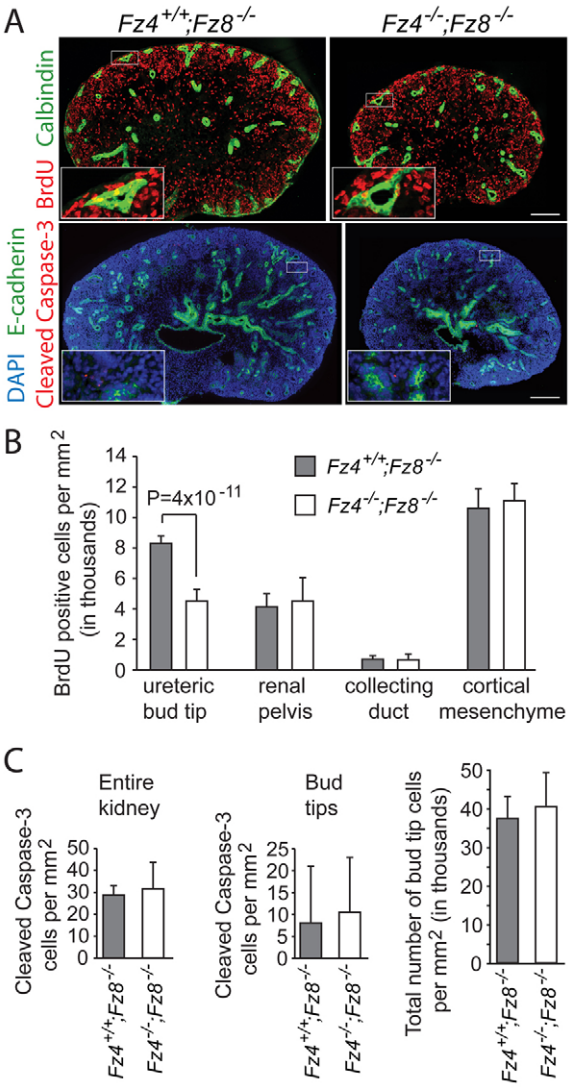

Fig. 4. Reduced cell proliferation accounts for the smaller size of *Fz4*$^{-/-}$;*Fz8*$^{-/-}$ mouse kidneys. (**A**) BrdU incorporation following a 1-hour pulse (top) and cleaved caspase 3 immunostaining (bottom) at E15. Insets show the boxed regions at higher magnification. Scale bars: 200 μm. (**B**) BrdU-labeled cells per mm^2 in the ureteric bud tips, renal pelvis, collecting duct (defined as the medullary region of the ureteric epithelium) and cortical mesenchyme. (**C**) Cleaved caspase 3 positive cells per mm^2 in the entire kidney or in the tips of the ureteric buds, and total cells per mm^2 in the tips of the ureteric buds. Mean + s.d. Twelve sections from four kidneys were analyzed.

(*Fz4*$^{AP/-}$;*Fz8*$^{-/-}$;*R26CreER*) and control (*Fz4*$^{AP/+}$;*Fz8*$^{-/-}$;*R26CreER*) embryos. A second assumption in these experiments is that loss of the Fz4 protein does not reduce expression at the *Fz4* promoter. If this assumption is valid then the absence of AP staining in the experimental kidneys implies an absence of *Fz4*$^{AP/-}$ cells. Fig. 5D shows one test of this assumption: a high dose (1 mg) of 4HT was delivered to the mother at E8.5 resulting in ~90% recombination in control (*Fz4*$^{AP/+}$;*Fz8*$^{-/-}$;*R26CreER*) kidneys at E12.5 and causing retarded ureteric bud development with retention of substantial numbers of AP-expressing *Fz4*$^{AP/-}$;*Fz8*$^{-/-}$ cells in all ureteric buds in the experimental (*Fz4*$^{AP/-}$;*Fz8*$^{-/-}$;*R26CreER*) kidneys. In a second test of this assumption, we directly compared the level of AP expression in *Fz4*$^{AP/+}$ and *Fz4*$^{AP/-}$ kidneys and found no differences (Fig. 5E).

It is interesting to note that there was only a small and statistically insignificant difference in the average number of terminal ureteric branches per kidney in a comparison between the two pairs of mosaic experimental and control kidneys at E12.5 (P>0.05; Student's t-test; Fig. 5C). The ~50% mosaicism seen in the control kidneys at E12.5 suggests that ~50% of the ureteric bud cells underwent Cre-mediated recombination in both control and experimental embryos at E8.5, and therefore that the phenotypically normal *Fz4*$^{CKOAP/-}$ cells in the experimental kidneys represented only ~50% of the ureteric epithelium immediately after Cre-mediated recombination. This line of reasoning implies that, in the mosaic ureteric epithelium of the experimental kidneys, phenotypically WT *Fz4*$^{CKOAP/-}$ cells exhibit an increase in proliferation relative to ureteric epithelial cells in control kidneys.

Gene expression changes in *Fz4*$^{-/-}$;*Fz8*$^{-/-}$ kidneys

To search for potential molecular mediators of Fz4 and Fz8 signaling in kidney development, we profiled the transcriptomes of *Fz4*$^{-/-}$;*Fz8*$^{-/-}$ versus *Fz4*$^{+/+}$;*Fz8*$^{-/-}$ and *Fz4*$^{-/-}$ versus WT kidneys at E13.5 by hybridization of three independent samples to Affymetrix MOE430 2.0 gene chips (Fig. 6). As expected, *Fz4* transcripts were substantially under-represented in the *Fz4*$^{-/-}$;*Fz8*$^{-/-}$ and *Fz4*$^{-/-}$ samples. In the *Fz4*$^{-/-}$;*Fz8*$^{-/-}$ versus *Fz4*$^{+/+}$;*Fz8*$^{-/-}$ comparison, but not the *Fz4*$^{-/-}$ versus WT comparison, a large number of transcripts exhibited greater than 2-fold abundance changes that were statistically significant (P<0.05).

Among the transcripts that exhibited a statistically significant decline in *Fz4*$^{-/-}$;*Fz8*$^{-/-}$ kidneys were those coding for Ret, Gfra1 and Gdnf (with declines estimated by chip hybridization of ~2-fold, ~2.5-fold and ~1.5-fold, respectively; Fig. 6A). As chip hybridization generally underestimates the fold reduction for rare transcripts owing to a non-zero background of nonspecific hybridization, we independently tested the abundance of *Gdnf* transcripts by in situ hybridization to E11.5 *Fz4*$^{-/-}$;*Fz8*$^{-/-}$ versus *Fz4*$^{+/+}$;*Fz8*$^{-/-}$ kidneys, a time point chosen to reveal differences in signaling components that would be predicted to determine ureteric bud growth and branching over the subsequent 1-2 days (Fig. 6A, inset). The in situ hybridization analysis revealed the previously described pattern of *Gdnf* expression within the mesenchyme that surrounds the ureteric bud in *Fz4*$^{+/+}$;*Fz8*$^{-/-}$ kidneys (Majumdar et al., 2003), and a large decrease in transcript abundance in *Fz4*$^{-/-}$;*Fz8*$^{-/-}$ kidneys relative to *Fz4*$^{+/+}$;*Fz8*$^{-/-}$ kidneys (n=4 experiments). These data suggest that part of the decrease in ureteric bud growth and branching in *Fz4*$^{-/-}$;*Fz8*$^{-/-}$ kidneys could be the result of a decrease in Gdnf levels and Gdnf-induced cell proliferation. We note that any decrease in Gdnf levels secondary to loss of Fz4 and Fz8 signaling is likely to be an indirect effect, as Gdnf is produced by the mesenchyme and Fz4 and Fz8 reside in the ureteric and nephron epithelia but not in the mesenchyme.

No statistically significant changes in *Gdnf*, *Ret* or *Gfra1* expression were detected in *Fz4*$^{-/-}$ kidneys compared with *Fz4*$^{+/+}$ control kidneys (Fig. 6B). In fact, the overall transcriptome profile of *Fz4*$^{-/-}$ kidneys closely resembled that of *Fz4*$^{+/+}$ kidneys, reflecting the relatively modest defect in kidney growth in *Fz4*$^{-/-}$ embryos.

Among the other transcripts with differential abundances in *Fz4*$^{-/-}$;*Fz8*$^{-/-}$ versus *Fz4*$^{+/+}$;*Fz8*$^{-/-}$ kidneys, transcript 5430421B17, a ~2.9 kb RNA of unknown function, was striking for its large decline in abundance in *Fz4*$^{-/-}$;*Fz8*$^{-/-}$ kidneys (Fig. 6A). This

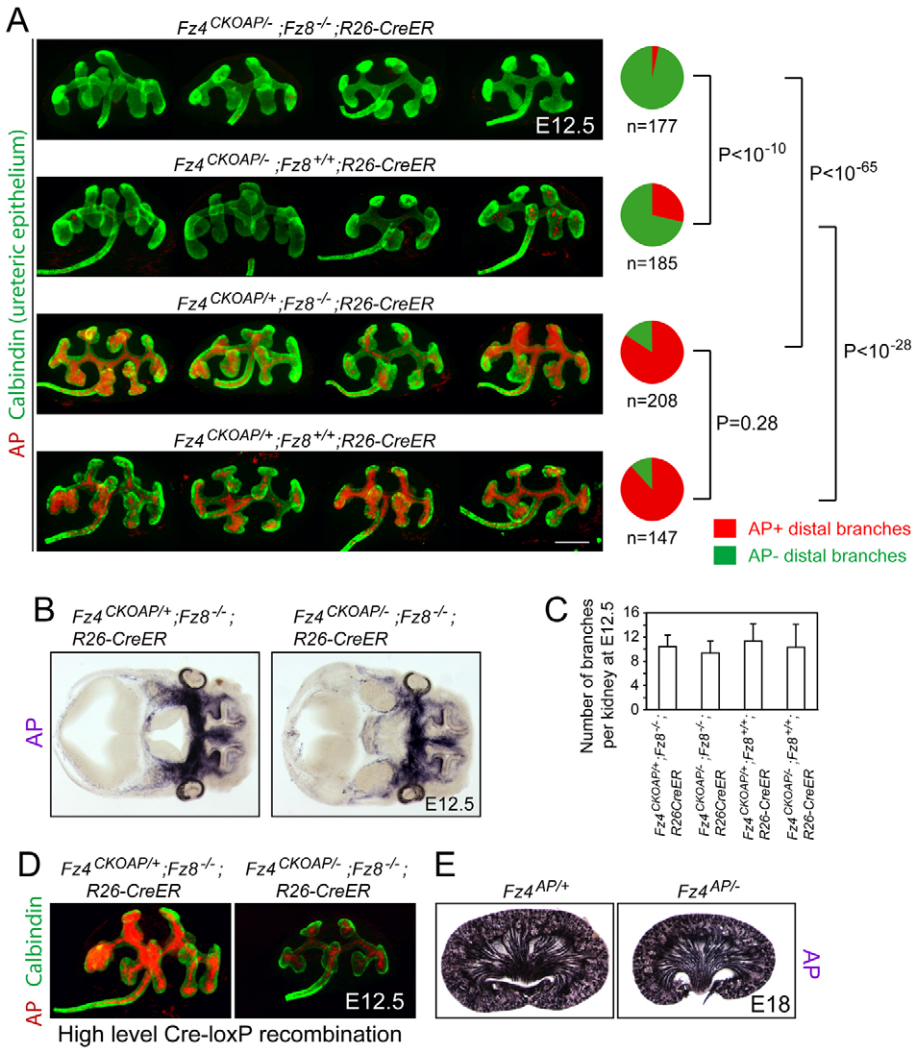

Fig. 5. Genetically marked *Fz4$^{AP/-}$* (i.e. *Fz4$^{-/-}$*) cells in mosaic ureteric epithelium are rapidly outgrown by their *Fz4$^{CKOAP/-}$* (i.e. *Fz4$^{+/-}$*) neighbors. (**A**) Whole-mount E12.5 mouse kidneys with AP^{+} cells visualized histochemically (false-colored red) and the ureteric epithelium visualized by calbindin immunostaining (green). Four representative kidneys are shown for each genotype. Embryos were exposed to 4-hydroxytamoxifen (4HT) at E8.5 via a single 200 μg subcutaneous injection into the dorsal fat pad of the mother. To the right is a quantification of the fraction of distal ureteric branches that contain any (red) or no (green) AP^{+} cells. Scale bar: 200 μm. (**B**) Histochemical stain for AP in 300 μm sections of the heads of E12.5 experimental and control littermates showing equal extents of Cre-mediated recombination at the *Fz4^{CKOAP}* allele. (**C**) Number of distal ureteric branches per kidney at E12.5 for the experiment in A. Mean + s.d. There is a small downward trend in the experimental groups in each pairwise comparison, but the differences between the two groups are statistically insignificant (P>0.05, Student's t-test). (**D**) As in A, except that 1 mg 4HT was delivered to the mother by oral gavage at E8.5, leading to ~90% *Fz4^{AP}* recombinant cells in E12.5 ureteric buds in the control kidney (left). The kidney with *Fz4$^{AP/-}$* cells (right) shows retarded ureteric bud growth and branching with some remaining AP^{+} cells. (**E**) E18 kidney sections stained histochemically for AP show that there is no decrease in expression of AP from the *Fz4* locus in the absence of *Fz4* function (*Fz4$^{AP/-}$* kidney, right panel).

transcript is located on mouse chromosome 7 between 85 bp and 3 kb 3′ of the *Fz4* gene and is transcribed from the same strand as the *Fz4* mRNA, suggesting that it derives from a longer variant of the *Fz4* transcript. Other transcripts with statistically significant abundance changes encode a highly diverse set of proteins (see Table S1 in the supplementary material).

Wnt11 as a candidate ligand for Fz4 and Fz8: canonical and noncanonical signaling

The phenotypes of reduced kidney size with preservation of renal architecture, diminished ureteric branching and reduced abundance of *Gdnf* transcripts that we observed in *Fz4$^{-/-}$;Fz8$^{-/-}$* embryos closely resemble those reported for *Wnt11$^{-/-}$* embryos (Majumdar et al., 2003). These similarities suggested that Fz4 and/or Fz8 might function as receptors for Wnt11 in kidney development.

Wnt11, along with Wnt5a, has been classified as a noncanonical Wnt based on its bioactivity in *Xenopus* embryos and the phenotype of the *silberblick* (*slb*) *wnt11* mutation in zebrafish (Heisenberg et al., 2000; Marlow et al., 2002; Veeman et al., 2003; Ulrich et al., 2005), but its roles in mammalian kidney and heart development are also compatible with it functioning as a canonical Wnt ligand (Majumdar et al., 2003; Nagy et al., 2010). To test the latter possibility, we used the Super Top Flash (STF) cell line to measure the Wnt11-, Fz4- and Fz8-dependence of transcriptional activation of a luciferase reporter under the control of a minimal promoter adjacent to seven LEF/TCF binding sites (Fig. 7A) (Xu et al., 2004). These experiments showed strong activation of canonical Wnt signaling that was dependent on ligand (Wnt11), receptor (Fz4) and co-receptor (Lrp5) (Fig. 7A, left). By contrast, Fz8 was unable to mediate Wnt11-dependent canonical signaling (Fig. 7A, right). As one control for the specificity of the assay, we observed the expected activation of canonical signaling when Norrin (the protein product of the Norrie disease gene, *Ndp*), an alternate Fz4 ligand, was substituted for Wnt11 (Fig. 7A, center). As a second control, we observed a decrease in signaling when the ligand-binding cysteine-rich domain (CRD) of Fz4 was co-expressed as a GPI-anchored protein (Fz4CRD-GPI); in this context, the CRD presumably acts as a competitive antagonist (Hsieh et al., 1999) (Fig. 7A, left and center).

Although Fz8 does not mediate Wnt11-dependent canonical signaling, we observed that co-expression of Fz8CRD-GPI more potently inhibits Wnt11/Fz4/Lrp5-mediated canonical signaling than does Fz4CRD-GPI (Fig. 7A, left panel). This inhibition is ligand-specific, as Fz8CRD-GPI did not inhibit Norrin/Fz4/Lrp5-mediated canonical signaling, consistent with the selectivity of Norrin for the Fz4 CRD over other Frizzled CRDs (Smallwood et al., 2007). Thus, these data indicate that both Fz4 and Fz8 CRDs can bind to Wnt11, but only Fz4 can mediate canonical signaling.

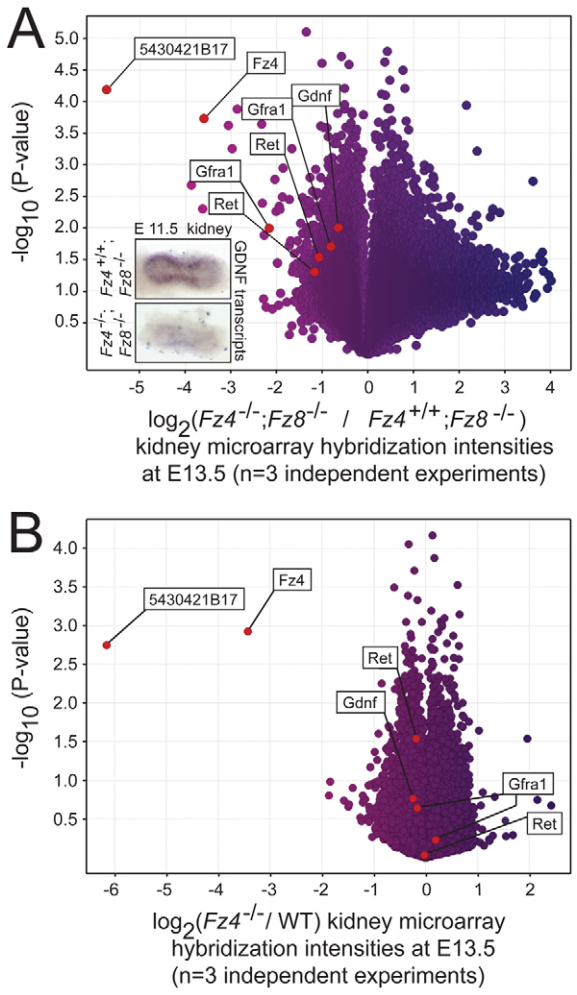

Fig. 6. Transcriptome changes in response to loss of *Fz4* with or without *Fz8*. (**A**,**B**) Mouse MOE430 2.0 Affymetrix arrays were hybridized in three biologically independent experiments with RNA from E13.5 *Fz4*$^{-/-}$;*Fz8*$^{-/-}$, *Fz4*$^{+/+}$;*Fz8*$^{-/-}$, *Fz4*$^{-/-}$ and WT kidneys (two to six kidneys per RNA sample). Probe sets representing *Ret*, *Gfra1* and *Gdnf* transcripts show reduced hybridization with RNA from *Fz4*$^{-/-}$;*Fz8*$^{-/-}$ kidneys. As expected, the probe set representing *Fz4* transcripts shows reduced hybridization with RNA from both sets of mutant kidneys. Insets in A show in situ hybridization of E11.5 kidneys, showing reduced levels of *Gdnf* transcripts in *Fz4*$^{-/-}$;*Fz8*$^{-/-}$ relative to *Fz4*$^{+/+}$;*Fz8*$^{-/-}$ kidneys.

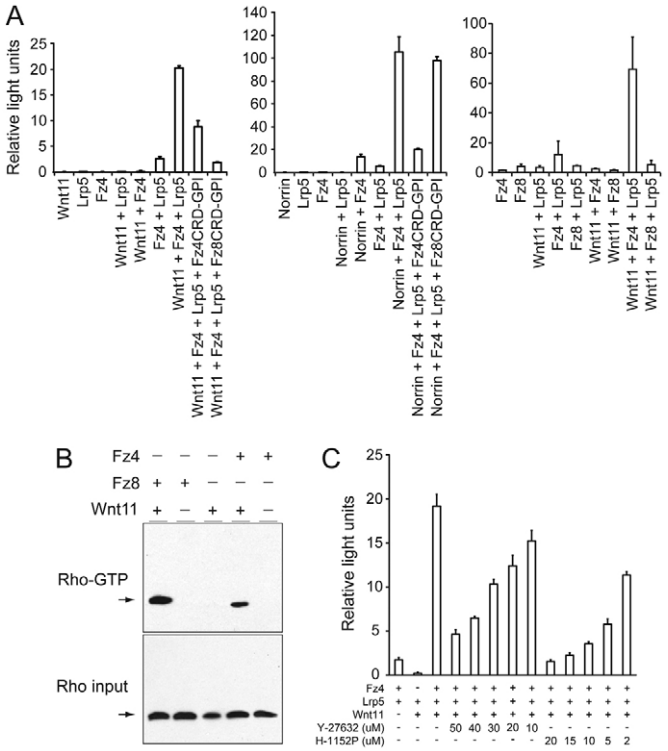

Fig. 7. Analysis of canonical and noncanonical Wnt signaling by Wnt11 via Fz4 and Fz8. (**A**) Luciferase assays for canonical Wnt signaling using transient transfection of STF cells with ligands (Wnt11 or Norrin), receptors (Fz4 or Fz8), co-receptor (Lrp5) and membrane-anchored competitors (Fz4CRD-GPI or Fz8CRD-GPI). Wnt11 activates canonical signaling via Fz4 and Lrp5 but not via Fz8 and Lrp5. (**B**) Increase in Rho-GTP concentration in transiently transfected HEK 293 cells in response to Wnt11 and Fz4 or Fz8. Immunoblots with anti-Rho antibodies showing GTP-bound Rho, captured with a GST-rhotekin fusion protein (upper panel), and total Rho in the postnuclear supernatant (lower panel). (**C**) Dose-dependent inhibition of canonical Wnt signaling in STF cells by Y-27632 and H-1152P, two inhibitors of Rho kinase (ROCK). Bar charts show mean + s.d. from triplicate experiments.

To test whether Wnt11 can activate noncanonical Wnt signaling via Fz4 and Fz8, we measured Rho activation in transiently transfected HEK 293 cells using a pulldown assay in which Rho-GTP, but not Rho-GDP, is selectively captured by the Rho-binding domain from rhotekin fused to glutathione-S-transferase (GST; Fig. 7B). This experiment showed that Wnt11 can induce noncanonical signaling via Fz4 or Fz8. The potential for Wnt11 to activate both canonical and noncanonical signaling in the same cell suggests that these pathways might interact either positively or negatively. Indeed, earlier work on inversin has suggested that in some cells there is a reciprocal relationship between canonical and noncanonical Wnt signaling (Simons et al., 2005). To explore this possibility, we asked whether pharmacological inhibition of Rho kinase (ROCK; a downstream mediator of Rho signaling) by either of two kinase inhibitors, Y-27632 and H-1152P (Ikenoya et al., 2002; Sasaki et al., 2002), could alter the magnitude of canonical Wnt signaling by Wnt11, Fz4 and Lrp5 in transiently transfected HEK 293 cells. Interestingly, both inhibitors showed a dose-dependent inhibition of canonical signaling (Fig. 7C), suggesting that, at least in this cellular context, there might be a synergy between these pathways such that canonical signaling is enhanced by the simultaneous activation of noncanonical signaling.

DISCUSSION

The experiments described here establish an essential role for Fz4 and Fz8 in controlling the size of the developing mammalian kidney. In particular, loss of *Fz4* and *Fz8* leads to retarded ureteric bud growth and branching, accompanied by decreased expression of *Gdnf*. The result is a small kidney of apparently normal

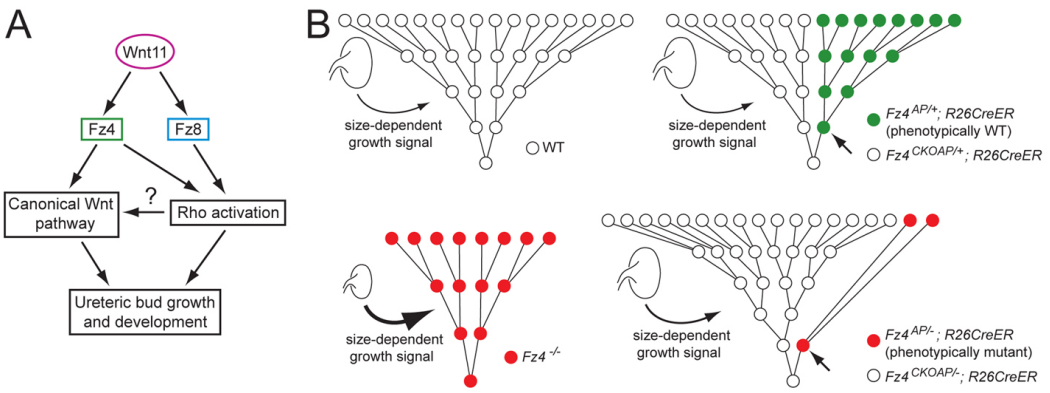

Fig. 8. Models of Wnt11 signaling and of cell proliferation and competition in the developing mouse kidney. (**A**) Wnt11 signals via Fz4 through both the canonical and noncanonical Wnt pathways, but via Fz8 only through the noncanonical pathway. (**B**) Inverted pyramids show several rounds of cell division during ureteric bud development. Time proceeds from bottom to top in each panel, and the relative rates of cell proliferation are reflected in the time between cell divisions. In WT kidneys (upper left) and in genetically mosaic kidneys (upper right), in which AP$^+$ cells (green) are phenotypically WT, cell proliferation is rapid and only a relatively weak kidney size-dependent growth-promoting signal further augments proliferation (thin curved arrow). In *Fz4*$^{-/-}$ or *Fz4*$^{-/-}$;*Fz8*$^{-/-}$ kidneys (lower left), reduced Wnt signaling leads to reduced cell proliferation, but this is partially compensated by strong activation of a kidney size-dependent growth-promoting signal (thick curved arrow). In genetically mosaic kidneys (lower right) in which marked cells (red) are *Fz4*$^{-/-}$ or *Fz4*$^{-/-}$;*Fz8*$^{-/-}$, the higher proliferation rate of phenotypically WT *Fz4*$^{+/-}$ or *Fz4*$^{+/-}$;*Fz8*$^{-/-}$ cells eventually leads to a predominantly WT ureteric bud. In this last situation, the model predicts that the kidney size-dependent growth-promoting signal would be only modestly activated (medium arrow), leaving the *Fz4*$^{-/-}$ or *Fz4*$^{-/-}$;*Fz8*$^{-/-}$ cells to proliferate at a greatly reduced rate. In each of the two right-hand diagrams, the small arrow points to the founder cell in the clone of Cre-recombined cells.

structure. These defects are consistent with a failure of Wnt11 signaling, which can activate canonical and noncanonical signaling via Fz4, but can only activate noncanonical signaling via Fz8 (Fig. 8A).

In genetic mosaics, marked ureteric bud cells lacking *Fz4* (in either a *Fz8*$^{+/+}$ or *Fz8*$^{-/-}$ background) are substantially underrepresented relative to neighboring cells that are heterozygous for *Fz4*. The magnitude of this proliferative (and/or survival) defect is far greater than one would have predicted based on the phenotype of mice in which *Fz4* is missing from all cells. The discrepancy could reflect the compensatory action of other growth regulatory circuits that together act to minimize the proliferative defects that arise from loss of Fz4 signaling (Fig. 8B). In developing kidneys composed entirely of phenotypically WT cells, this model posits that the compensatory growth-promoting signals would be minimally active (Fig. 8B, upper two panels). By contrast, in genetically homogeneous *Fz4*$^{-/-}$ kidneys, one would expect that compensatory signals would be highly active, although they are insufficient to fully correct the cell proliferation defect (Fig. 8B, lower left). In genetically mosaic kidneys, the compensatory signals would be modestly active, thereby driving an expansion of the pool of phenotypically WT *Fz4*$^{+/-}$ cells relative to their slow-growing *Fz4*$^{-/-}$ neighbors (Fig. 8B, lower right).

A potential explanation for the differential abundances of *Fz4*$^{+/-}$ and *Fz4*$^{-/-}$ cells in mosaic kidneys is a primary defect in cell behavior that secondarily results in differential cell proliferation, rather than there being intrinsic differences in the rates of proliferation. In fact, within the caudal Wolffian duct there is precedent for a Ret-dependent competitive interaction between neighboring cells that produces both differential cell migration and differential cell proliferation. In chimeric WT:*Ret*$^{-/-}$ embryos, WT cells preferentially occupy the proliferative domain associated with the primary ureteric bud tip and *Ret*$^{-/-}$ cells are excluded from it (Shakya et al., 2005; Chi et al., 2009). As a result, in the late-gestation kidney, WT cells dominate the distal branches of the ureteric epithelium and *Ret*$^{-/-}$ cells are largely confined to the proximal branches. This differential migration and proliferation mechanism could plausibly account for the dramatic difference in the abundance of *Fz4*$^{+/-}$ versus *Fz4*$^{-/-}$ (or of *Fz4*$^{+/-}$;*Fz8*$^{-/-}$ versus *Fz4*$^{-/-}$;*Fz8*$^{-/-}$) cells that we observed in mosaic E12.5 kidneys following Cre-mediated recombination at E8.5. It is unclear whether this mechanism could also account for the differential proliferation of ureteric bud tips in non-mosaic *Fz4*$^{+/+}$;*Fz8*$^{-/-}$ versus *Fz4*$^{-/-}$;*Fz8*$^{-/-}$ kidneys at E15.5 (Fig. 4), a situation in which no competition occurs and the mutant cells occupy all positions within the ureteric bud.

We note that the 'migration controls proliferation' mechanism described above is not conceptually at odds with the general feedback model depicted in Fig. 8. If cell proliferation is determined by cell location, then controlling cell migration is one specific mechanism by which cell proliferation could be regulated by a feedback signal.

Regulatory networks for growth control in kidney development

The present work fills in one missing piece in the complex network of cell regulatory signals that coordinate early kidney development. Of particular interest is the prediction that Fz4 and Fz8 loss-of-function mutations decrease the level of Gdnf/Ret/Gfra1 signaling, as judged by the decrease in *Gdnf*, *Ret* and *Gfra1* transcripts in *Fz4*$^{-/-}$;*Fz8*$^{-/-}$ kidneys. Proliferative defects in both Wnt and RA signaling mutants appear to reflect, at least in part, downregulation of Gdnf signaling. With respect to RA signaling, *RARalpha*$^{-/-}$;*RARbeta2*$^{-/-}$ (*Rara*$^{-/-}$;*Rarb*$^{-/-}$) mice exhibit a hypoplastic kidney phenotype with downregulation of *Ret* transcripts. This phenotype can be reversed by forced expression of *Ret* in the ureteric epithelium (Mendelsohn et al., 1999; Batourina et al., 2001). A similar phenotype is produced by expression of a dominant-negative RA receptor in ureteric buds, which also leads to downregulation of Ret (Rosselot et al., 2010).

Gdnf signaling in the context of ureteric bud growth is also modulated by BMP/Gremlin and Jagged/Notch signaling (Kuure et al., 2005; Michos et al., 2004; Michos et al., 2007).

As noted above, the competitive disadvantage exhibited by *Fz4*$^{-/-}$ relative to *Fz4*$^{+/-}$ ureteric bud cells (either with or without *Fz8* function) is reminiscent of the competitive disadvantage exhibited by *Ret*$^{-/-}$ relative to WT ureteric bud cells (Shakya et al., 2005; Chi et al., 2009). The reduced expression of *Gdnf* and *Ret* that we observe in *Fz4*$^{-/-}$;*Fz8*$^{-/-}$ kidneys suggests that the under-representation of *Fz4*$^{-/-}$ relative to *Fz4*$^{+/-}$ cells in mosaic E12.5 ureteric buds could arise, at least in part, from a defect in the Gdnf/Ret-dependent tip-cell developmental pathway defined by Shakya et al. (Shakya et al., 2005) and Chi et al. (Chi et al., 2009).

The relative contributions of canonical and noncanonical Wnt signaling to different aspects of kidney development are still largely unexplored. Wnt9b has been inferred to act via canonical Wnt signaling to induce differentiation of the metanephric mesenchyme based on the ability of Wnt1, a canonical Wnt, to functionally substitute for it (Carroll et al., 2005). Noncanonical/planar cell polarity signaling orients cell divisions along the long axis of renal tubules and derangements in this system are implicated in some cystic kidney disease (Simons and Walz, 2006; Saburi et al., 2008; Bacallao and McNeill, 2009). In the case of Wnt11, the present work indicates that both canonical and noncanonical pathways are potentially operative. The data also suggest that the distinction between canonical and noncanonical Wnt ligands might be less clear-cut than previously assumed and that, depending on the particular Wnt and Frizzled (or non-Frizzled) receptor, the downstream pathway might vary.

Redundancy and robustness in cell signaling pathways

Robustness – the characteristic of resilience in the face of perturbation – is one of the hallmarks of complex biological systems. In vertebrate physiology, homeostatic control of blood pressure, pH and oxygen tension represent classic examples in which tissue health is maintained by multiple feedback loops that adjust respiration rate, heart rate, vascular tone and renal function on a time scale of seconds to hours. Homeostatic mechanisms also operate on time scales of days to years by adjusting red cell production, myocardial and vascular growth and/or renal function, as seen in the chronic responses to hypertension, hypoxia or nephrectomy (Wakatsuki et al., 2004; Ibrahim et al., 2009; Rey and Semenza, 2010). Robustness in the context of embryonic development presents a potentially greater challenge to the organism because compensatory responses must occur rapidly so that different developmental events are not desynchronized.

Genetic redundancy is a well-known strategy for achieving developmental robustness when the perturbation is genetic variation. For diploid organisms, the presence of a second allele confers a minimal level of redundancy. A further level of genetic redundancy can arise from the partially overlapping functions of closely related members of gene families. A more sophisticated strategy for achieving developmental robustness in the face of either genetic or environmental perturbation involves the evolution of signaling systems that refine the rates of cell proliferation, differentiation and survival to match local requirements, where ‘local’ refers to both space and time. Examples include the regulation of embryonic vascular growth by hypoxia inducible factor (HIF) and vascular endothelial growth factor (VEGF) in response to tissue oxygen demand (Rey and Semenza, 2010), and the regulation of neuronal cell death in the dorsal root ganglion by limiting quantities of target-derived trophic signals, such as nerve growth factor (Levi-Montalcini, 1966).

In the present instance, each of the three strategies described above appears to be operating: (1) *Fz4* is recessive (allelic compensation); (2) *Fz4* and *Fz8* are partially redundant (locus compensation); and (3) in the absence of *Fz4* and *Fz8*, the kidney phenotype appears to be partly ameliorated by the compensatory actions of other regulatory systems (pathway compensation). With respect to the third strategy, the genetic mosaic experiments show that failure of Fz4/Fz8 signaling in ~50% of ureteric bud epithelial cells has little or no effect on the overall rate of ureteric bud growth and branching and no effect on the postnatal survival of the mice. A strikingly similar observation has been made in the context of Fgfr2 signaling in mouse mammary epithelial cells: when a mixture of genetically marked *Fgfr2*$^{+/-}$ and *Fgfr2*$^{-/-}$ mammary epithelial cells is implanted into a fat pad, the ducts that develop over the ensuing weeks are composed almost exclusively of *Fgfr2*$^{+/-}$ cells (Lu et al., 2008). It would be of interest to extend this observation by determining whether, in its normal developmental context, a pure population of *Fgfr2*$^{-/-}$ mammary epithelial cells could grow into a mature duct.

Genetic mosaic approaches in mammalian developmental genetics

Genetic mosaic methods in which individual WT and mutant cells are distinguished by visible markers are rarely used in studies of mammalian development but have been widely used in *Drosophila* (Simpson, 1976; Wu and Luo, 2006; Potter et al., 2010). Arranging for the coincident deletion (or some other alteration) in the gene of interest and activation of a fluorescent, histochemical or immunohistochemical reporter presents a distinct technical challenge in mammalian systems. In the *Drosophila* MARCM system, this coincidence is effected by a single Flp-mediated recombination event at the base of a chromosome arm. The small number of *Drosophila* chromosomes (four), together with the availability of balancer chromosomes, facilitates this approach. Although an analogous approach based on Cre-mediated mitotic recombination has been developed in the mouse (Zong et al., 2005), generalizing it to all chromosome arms will be challenging. Alternative approaches are exemplified by the embryo chimera experiments of Chi et al. (Chi et al., 2009) and by the present work, which is based on a conditional allele that couples deletion of the coding region of interest to the activation of a previously silent reporter gene (Fleischmann et al., 2003; Liu et al., 2008; Badea et al., 2009; Ye et al., 2009). These and other approaches for the activation or inactivation of genes in genetically marked cells should eventually make mosaic analysis a more accessible tool for the study of mammalian developmental biology.

Acknowledgements

We thank Haiping Hao and Connie Talbot for microarray support; Aurora Esquela, David Ginty and Wenqin Luo for plasmids; and Max Tischfield and two anonymous referees for helpful comments on the manuscript. Supported by the Howard Hughes Medical Institute and the National Eye Institute (NIH). Deposited in PMC for release after 6 months.

Competing interests statement

The authors declare no competing financial interests.

Supplementary material

Supplementary material for this article is available at
http://dev.biologists.org/lookup/suppl/doi:10.1242/dev.057620/-/DC1

References

Bacallao, R. L. and McNeill, H. (2009). Cystic kidney diseases and planar cell polarity signaling. *Clin. Genet.* **75**, 107-117.

Badea, T. C., Wang, Y. and Nathans, J. (2003). A noninvasive genetic/pharmacologic strategy for visualizing cell morphology and clonal relationships in the mouse. *J. Neurosci.* **23**, 2314-2322.

Badea, T. C., Cahill, H., Ecker, J., Hattar, S. and Nathans, J. (2009). Distinct roles of transcription factors brn3a and brn3b in controlling the development, morphology, and function of retinal ganglion cells. *Neuron* **61**, 852-864.

Basson, M. A., Watson-Johnson, J., Shakya, R., Akbulut, S., Hyink, D., Costantini, F. D., Wilson, P. D., Mason, I. J. and Licht, J. D. (2006). Branching morphogenesis of the ureteric epithelium during kidney development is coordinated by the opposing functions of GDNF and Sprouty1. *Dev. Biol.* **299**, 466-477.

Bates, C. M. (2007). Role of fibroblast growth factor receptor signaling in kidney development. *Pediatr. Nephrol.* **22**, 343-349.

Batourina, E., Gim, S., Bello, N., Shy, M., Clagett-Dame, M., Srinivas, S., Costantini, F. and Mendelsohn, C. (2001). Vitamin A controls epithelial/mesenchymal interactions through Ret expression. *Nat. Genet.* **27**, 74-78.

Brenner, B. M. and Mackenzie, H. S. (1997). Nephron mass as a risk factor for progression of renal disease. *Kidney Int.* **63**, S124-S127.

Carroll, T. J., Park, J. S., Hayashi, S., Majumdar, A. and McMahon, A. P. (2005). Wnt9b plays a central role in the regulation of mesenchymal to epithelial transitions underlying organogenesis of the mammalian urogenital system. *Dev. Cell* **9**, 283-292.

Chi, L., Zhang, S., Lin, Y., Prunskaite-Hyyryläinen, R., Vuolteenaho, R., Itäranta, P. and Vainio, S. (2004). Sprouty proteins regulate ureteric branching by coordinating reciprocal epithelial Wnt11, mesenchymal Gdnf and stromal Fgf7 signalling during kidney development. *Development* **131**, 3345-3356.

Chi, X., Michos, O., Shakya, R., Riccio, P., Enomoto, H., Licht, J. D., Asai, N., Takahashi, M., Ohgami, N., Kato, M. et al. (2009). Ret-dependent cell rearrangements in the Wolffian duct epithelium initiate ureteric bud morphogenesis. *Dev. Cell* **17**, 199-209.

Costantini, F. and Shakya, R. (2006). GDNF/Ret signaling and the development of the kidney. *BioEssays* **28**, 117-127.

Dressler, G. R. (2009). Advances in early kidney specification, development, and patterning. *Development* **136**, 3863-3874.

Fleischmann, A., Hvalby, O., Jensen, V., Strekalova, T., Zacher, C., Layer, L. E., Kvello, A., Reschke, M., Spanagel, R., Sprengel, R. et al. (2003). Impaired long-term memory and NR2A-type NMDA receptor-dependent synaptic plasticity in mice lacking c-Fos in the CNS. *J. Neurosci.* **23**, 9116-9122.

Giral, M., Foucher, Y., Karam, G., Labrune, Y., Kessler, M., de Ligny, B. H., Büchler, M., Bayle, F., Meyer, C., Trehet, N. et al. (2010). Kidney and recipient weight incompatibility reduces long-term graft survival. *J. Am. Soc. Nephrol.* **21**, 1022-1029.

Godin, R. E., Robertson, E. J. and Dudley, A. T. (1999). Role of BMP family members during kidney development. *Int. J. Dev. Biol.* **43**, 405-411.

Grieshammer, U., Cebrián, C., Ilagan, R., Meyers, E., Herzlinger, D. and Martin, G. R. (2005). FGF8 is required for cell survival at distinct stages of nephrogenesis and for regulation of gene expression in nascent nephrons. *Development* **132**, 3847-3857.

Heisenberg, C. P., Tada, M., Rauch, G. J., Saúde, L., Concha, M. L., Geisler, R., Stemple, D. L., Smith, J. C. and Wilson, S. W. (2000). Silberblick/Wnt11 mediates convergent extension movements during zebrafish gastrulation. *Nature* **405**, 76-81.

Hellmich, H. L., Kos, L., Cho, E. S., Mahon, K. A. and Zimmer, A. (1996). Embryonic expression of glial cell-line derived neurotrophic factor (GDNF) suggests multiple developmental roles in neural differentiation and epithelial-mesenchymal interactions. *Mech. Dev.* **54**, 95-105.

Hsieh, J. C., Rattner, A., Smallwood, P. M. and Nathans, J. (1999). Biochemical characterization of Wnt-frizzled interactions using a soluble, biologically active vertebrate Wnt protein. *Proc. Natl. Acad. Sci. USA* **96**, 3546-3551.

Ibrahim, H. N., Foley, R., Tan, L., Rogers, T., Bailey, R. F., Guo, H., Gross, C. R. and Matas, A. J. (2009). Long-term consequences of kidney donation. *N. Engl. J. Med.* **360**, 459-469.

Ikenoya, M., Hidaka, H., Hosoya, T., Suzuki, M., Yamamoto, N. and Sasaki, Y. (2002). Inhibition of rho-kinase-induced myristoylated alanine-rich C kinase substrate (MARCKS) phosphorylation in human neuronal cells by H-1152, a novel and specific Rho-kinase inhibitor. *J. Neurochem.* **81**, 9-16.

Kuure, S., Sainio, K., Vuolteenaho, R., Ilves, M., Wartiovaara, K., Immonen, T., Kvist, J., Vainio, S. and Sariola, H. (2005). Crosstalk between Jagged1 and GDNF/Ret/GFRalpha1 signalling regulates ureteric budding and branching. *Mech. Dev.* **122**, 765-780.

Levi-Montalcini, R. (1966). The nerve growth factor: its mode of action on sensory and sympathetic nerve cells. *Harvey Lect.* **60**, 217-259.

Liu, C., Wang, Y., Smallwood, P. M. and Nathans, J. (2008). An essential role for Frizzled5 in neuronal survival in the parafascicular nucleus of the thalamus. *J. Neurosci.* **28**, 5641-5653.

Lu, P., Ewald, A. J., Martin, G. R. and Werb, Z. (2008). Genetic mosaic analysis reveals FGF receptor 2 function in terminal end buds during mammary gland branching morphogenesis. *Dev. Biol.* **321**, 77-87.

Majumdar, A., Vainio, S., Kispert, A., McMahon, J. and McMahon, A. P. (2003). Wnt11 and Ret/Gdnf pathways cooperate in regulating ureteric branching during metanephric kidney development. *Development* **130**, 3175-3185.

Marlow, F., Topczewski, J., Sepich, D. and Solnica-Krezel, L. (2002). Zebrafish Rho kinase 2 acts downstream of Wnt11 to mediate cell polarity and effective convergence and extension movements. *Curr. Biol.* **12**, 876-884.

Martín, F. A. and Morata, G. (2006). Compartments and the control of growth in the Drosophila wing imaginal disc. *Development* **133**, 4421-4426.

McMahon, A. P., Aronow, B. J., Davidson, D. R., Davies, J. A., Gaido, K. W., Grimmond, S., Lessard, J. L., Little, M. H., Potter, S. S., Wilder, E. L. et al. (2008). GUDMAP: the genitourinary developmental molecular anatomy project. *J. Am. Soc. Nephrol.* **19**, 667-671.

Mendelsohn, C., Batourina, E., Fung, S., Gilbert, T. and Dodd, J. (1999). Stromal cells mediate retinoid-dependent functions essential for renal development. *Development* **126**, 1139-1148.

Michos, O., Panman, L., Vintersten, K., Beier, K., Zeller, R. and Zuniga, A. (2004). Gremlin-mediated BMP antagonism induces the epithelial-mesenchymal feedback signaling controlling metanephric kidney and limb organogenesis. *Development* **131**, 3401-3410.

Michos, O., Gonçalves, A., Lopez-Rios, J., Tiecke, E., Naillat, F., Beier, K., Galli, A., Vainio, S. and Zeller, R. (2007). Reduction of BMP4 activity by gremlin 1 enables ureteric bud outgrowth and GDNF/WNT11 feedback signalling during kidney branching morphogenesis. *Development* **134**, 2397-2405.

Migeon, B. R. (1998). Non-random X chromosome inactivation in mammalian cells. *Cytogenet. Cell Genet.* **80**, 142-148.

Nagy, I. I., Railo, A., Rapila, R., Hast, T., Sormunen, R., Tavi, P., Räsänen, J. and Vainio, S. J. (2010). Wnt-11 signalling controls ventricular myocardium development by patterning N-cadherin and beta-catenin expression. *Cardiovasc. Res.* **85**, 100-109.

Neto-Silva, R. M., Wells, B. S. and Johnston, L. A. (2009). Mechanisms of growth and homeostasis in the Drosophila wing. *Annu. Rev. Cell Dev. Biol.* **25**, 197-220.

Otsu, M., Sugamura, K. and Candotti, F. (2000). In vivo competitive studies between normal and common gamma chain-defective bone marrow cells: implications for gene therapy. *Hum. Gene Ther.* **11**, 2051-2056.

Oxburgh, L., Chu, G. C., Michael, S. K. and Robertson, E. J. (2004). TGFbeta superfamily signals are required for morphogenesis of the kidney mesenchyme progenitor population. *Development* **131**, 4593-4605.

Potter, C. J., Tasic, B., Russler, E. V., Liang, L. and Luo, L. (2010). The Q system: a repressible binary system for transgene expression, lineage tracing, and mosaic analysis. *Cell* **141**, 536-348.

Rey, S. and Semenza, G. L. (2010). Hypoxia-inducible factor-1-dependent mechanisms of vascularization and vascular remodelling. *Cardiovasc. Res.* **86**, 236-242.

Rosselot, C., Spraggon, L., Chia, I., Batourina, E., Riccio, P., Lu, B., Niederreither, K., Dolle, P., Duester, G., Chambon, P. et al. (2010). Non-cell-autonomous retinoid signaling is crucial for renal development. *Development* **137**, 283-292.

Saburi, S., Hester, I., Fischer, E., Pontoglio, M., Eremina, V., Gessler, M., Quaggin, S. E., Harrison, R., Mount, R. and McNeill, H. (2008). Loss of Fat4 disrupts PCP signaling and oriented cell division and leads to cystic kidney disease. *Nat. Genet.* **40**, 1010-1015.

Salic, A. and Mitchison, T. J. (2008). A chemical method for fast and sensitive detection of DNA synthesis in vivo. *Proc. Natl. Acad. Sci. USA* **105**, 2415-2420.

Sasaki, Y., Suzuki, M. and Hidaka, H. (2002). The novel and specific Rho-kinase inhibitor (S)-(+)-2-methyl-1-[(4-methyl-5-isoquinoline)sulfonyl]-homopiperazine as a probing molecule for Rho-kinase-involved pathway. *Pharmacol. Ther.* **93**, 225-232.

Schaeren-Wiemers, N. and Gerfin-Moser, A. (1993). A single protocol to detect transcripts of various types and expression levels in neural tissue and cultured cells: in situ hybridization using digoxigenin-labelled cRNA probes. *Histochemistry* **100**, 431-440.

Shakya, R., Watanabe, T. and Costantini, F. (2005). The role of GDNF/Ret signaling in ureteric bud cell fate and branching morphogenesis. *Dev. Cell* **8**, 65-74.

Simons, M. and Walz, G. (2006). Polycystic kidney disease: cell division without a c(l)ue? *Kidney Int.* **70**, 854-864.

Simons, M., Gloy, J., Ganner, A., Bullerkotte, A., Bashkurov, M., Krönig, C., Schermer, B., Benzing, T., Cabello, O. A., Jenny, A. et al. (2005). Inversin, the gene product mutated in nephronophthisis type II, functions as a molecular switch between Wnt signaling pathways. *Nat. Genet.* **37**, 537-543.

Simpson, P. (1976). Analysis of the compartments of the wing of Drosophila melanogaster mosaic for a temperature-sensitive mutation that reduces mitotic rate. *Dev. Biol.* **54**, 100-115.

Smallwood, P. M., Williams, J., Xu, Q., Leahy, D. J. and Nathans, J. (2007). Mutational analysis of Norrin-Frizzled4 recognition. *J. Biol. Chem.* **282**, 4057-4068.
Song, R., Spera, M., Garrett, C., El-Dahr, S. S. and Yosypiv, I. V. (2010). Angiotensin II AT2 receptor regulates ureteric bud morphogenesis. *Am. J. Physiol. Renal Physiol.* **298**, F807-F817.
Stark, K., Vainio, S., Vassileva, G. and McMahon, A. P. (1994). Epithelial transformation of metanephric mesenchyme in the developing kidney regulated by Wnt-4. *Nature* **372**, 679-683.
Ulrich, F., Krieg, M., Schötz, E. M., Link, V., Castanon, I., Schnabel, V., Taubenberger, A., Mueller, D., Puech, P. H. and Heisenberg, C. P. (2005). Wnt11 functions in gastrulation by controlling cell cohesion through Rab5c and E-cadherin. *Dev. Cell* **9**, 555-564.
van Amerongen, R. and Nusse, R. (2009). Towards an integrated view of Wnt signaling in development. *Development* **136**, 3205-3214.
Veeman, M. T., Axelrod, J. D. and Moon, R. T. (2003). A second canon. Functions and mechanisms of beta-catenin-independent Wnt signaling. *Dev. Cell* **5**, 367-377.
Vulliamy, T. J., Knight, S. W., Dokal, I. and Mason, P. J. (1997). Skewed X-inactivation in carriers of X-linked dyskeratosis congenita. *Blood* **90**, 2213-2216.
Wakatsuki, T., Schlessinger, J. and Elson, E. L. (2004). The biochemical response of the heart to hypertension and exercise. *Trends Biochem. Sci.* **29**, 609-617.
Wang, Y., Huso, D., Cahill, H., Ryugo, D. and Nathans, J. (2001). Progressive cerebellar, auditory, and esophageal dysfunction caused by targeted disruption of the frizzled-4 gene. *J. Neurosci.* **21**, 4761-4771.
Weinberg, R. A. (2006). *The Biology of Cancer.* London: Garland Science.
Wu, J. S. and Luo, L. (2006). A protocol for mosaic analysis with a repressible cell marker (MARCM) in Drosophila. *Nat. Protoc.* **1**, 2583-2589.
Xu, Q., Wang, Y., Dabdoub, A., Smallwood, P. M., Williams, J., Woods, C., Kelley, M. W., Jiang, L., Tasman, W., Zhang, K. et al. (2004). Vascular development in the retina and inner ear: control by Norrin and Frizzled-4, a high-affinity ligand-receptor pair. *Cell* **116**, 883-895.
Ye, X., Wang, Y., Cahill, H., Yu, M., Badea, T. C., Smallwood, P. M., Peachey, N. S. and Nathans, J. (2009). Norrin, frizzled-4, and Lrp5 signaling in endothelial cells controls a genetic program for retinal vascularization. *Cell* **139**, 285-298.
Zong, H., Espinosa, J. S., Su, H. H., Muzumdar, M. D. and Luo, L. (2005). Mosaic analysis with double markers in mice. *Cell* **121**, 479-492.